A Continuum Body Force Sensor Designed for Flexible Surgical Robotics Devices

Yohan Noh, *IEEE Member*, Emanuele Lindo Secco, Sina Sareh, Helge Würdemann, Angela Faragasso, Junghwan Back, Hongbin Liu, *IEEE Member*, Elizabeth Sklar, Kaspar Althoefer, *IEEE Member*

***Abstract*— This paper presents a novel three-axis force sensor based on optical photo interrupters and integrated with the robot arm STIFF-FLOP (STIFFness controllable Flexible and Learnable Manipulator for Surgical Operations) to measure external interacting forces and torques. The ring-shape bio-compatible sensor presented here embeds the distributed actuation and sensing system of the STIFF-FLOP manipulator and is applicable to the geometry of its structure as well to the structure of any other similar soft robotic manipulator. Design and calibration procedures of the device are introduced: experimental results allow defining a stiffness sensor matrix for real-time estimation of force and torque components and confirm the usefulness of the proposed optical sensing approach.**

I. Introduction

During surgical operation, robotic technology can provide valuable assistance for surgical procedures. For example, the da Vinci Surgical System (http://www.davincisurgery.com/) is a popular surgical robot for MIS (Minimally Invasive Surgery). The robot arm of the da Vinci has multiple degrees of freedom (DoF), which makes it easier to carry out surgical operations in a restricted environment. The 3D camera of the da Vinci provides enlarged detail visual information on the surgical site. However, its robot arm has the following shortcomings: 1) the small workspace of its robot arm is constrained by rigid mechanical links; and 2) information describing the interaction between the robot's arms and the patient's organs is not provided during a surgical procedure.

In order to overcome the shortcomings of conventional medical devices, as well as those of surgical robots—particularly of those that are composed of rigid links—the scientific community has started developing a new class of flexible manipulators. In 2009, Simaan *et al.*, Alexander *et al.*, and Taylor *et al.* presented dexterous, flexible snake-like manipulators that can provide relatively high dexterity and mobility in narrow anatomical areas not easily accessible by traditional robotic instruments [1-3]. Rucker *et al.* developed active cannula manipulators, which are a new class of thin, dexterous and continuum robots, capable of accessing narrow openings, such as the throat and lung [4]. More recently, Cheng et al., Jiang et al., and Breedveld et al. developed flexible manipulators, which can even change their stiffness and are capable of dexterous precise motion control by cables [5-7]. Nevertheless, in most of these surgical robotic devices the incorporation of sensors able to provide information about the effective pose of the robot and the physical interactions with the surrounding environment has been neglected.

For these reasons, the EU-funded project STIFF-FLOP was proposed in 2012 [8]. The STIFF-FLOP arm (Figure 1) is a soft robotic arm which can squeeze through standard Trocar ports and can then be controlled, achieving omni-elongation and bending of the arm by using air pressure for actuation. Integrated sensors are used for perception of mechanical interaction with the environment and providing feedback. An important aspect of this sensor system is its capability to measure the force and torque information through integrated sensors. In addition, inside the arm, a stiffening chamber

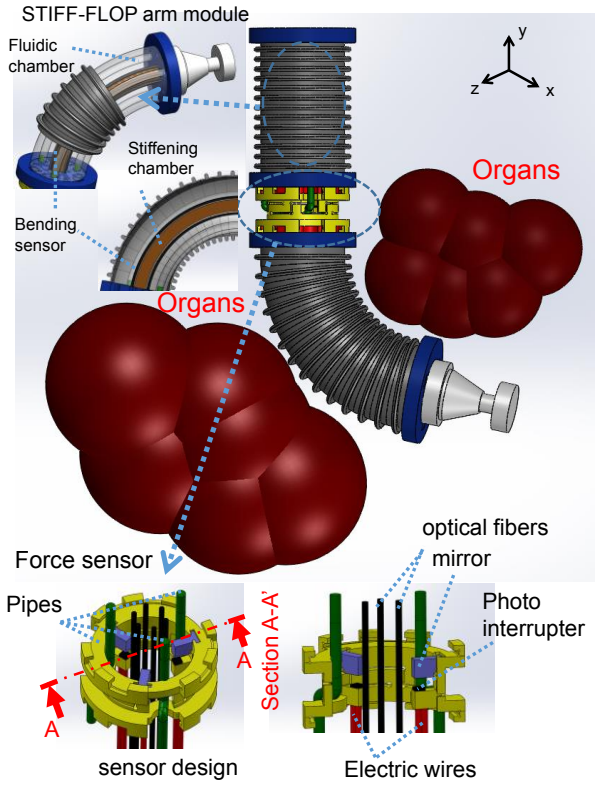

Figure 1. Overview of the STIFF-FLOP manipulator and three axis force sensor based on photo interrupters

Manuscript received April 7th, 2014. The research leading to these results has received funding from the European Commission's Seventh Framework Programme; project STIFF-FLOP (Grant No: 287728).

Yohan Noh (corresponding author, email: yohan.noh@kcl.ac.uk), Emanuele Lindo Secco, Sina Sareh, Helge Würdemann, Angela Faragasso, Junghwan Back, Hongbin Liu, and Kaspar Althoefer are with King's College London, School of Natural and Mathematical Sciences, Department of Informatics, UK.

Elizabeth Sklar is with the Department of Computer Science, University of Liverpool, UK.

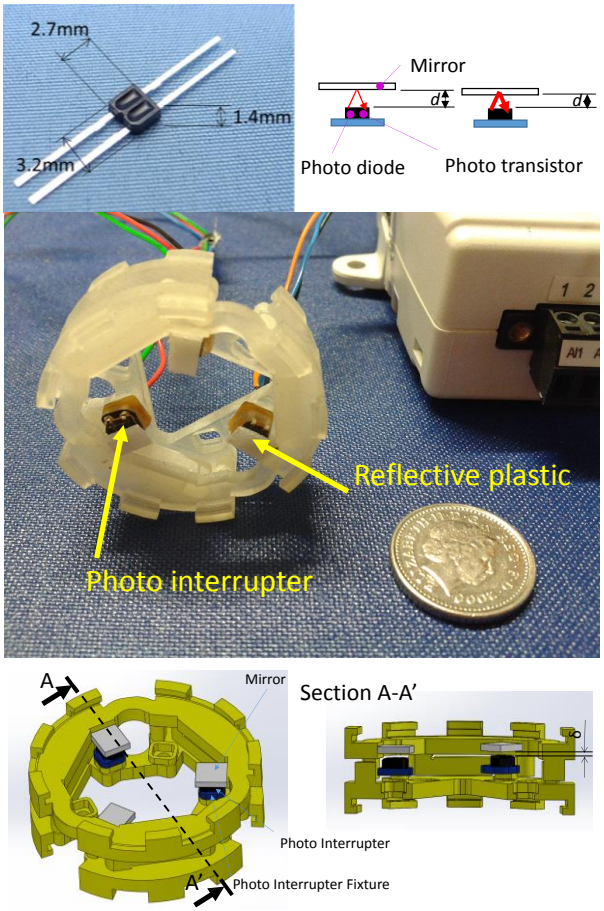

Figure 2. Photo interrupter (top panels) and three axis force sensor (central and bottom panels) with 3 integrated photo interrupters.

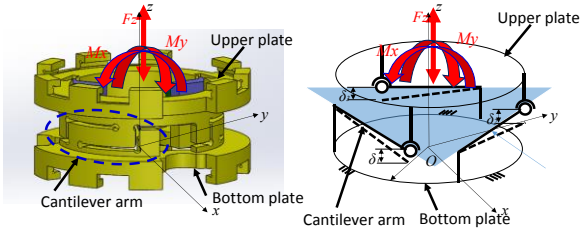

Figure 3. Sensor operating principle based on 3 flexible cantilever beams

enables tightening and compliant force control [9-11].

In general, many robots for industrial and medical applications use multi-axial force sensors, which are based on strain gauges that measure force and torque. Unfortunately, these types of sensors cannot be easily integrated within dexterous continuum robots such as the STIFF-FLOP manipulator: in fact, the structure of a strain gauge is normally filled with solid material that does not allow pipes and cables to pass through, in contrast to the STIFF-FLOP design, which features a hollow core to allow passage of components such as optical fibres (Figure 1).

Therefore, a ring-shaped multi-axial force sensor, based on a hollowed structure, is proposed here. The sensor can be integrated with the STIFF-FLOP arm and with many other dexterous continuum robots where two (or more) elements are linked via rigid joints. In contrast with multi-axial force sensors based on strain gauge technology, this novel device takes advantage of the use of optoelectronic components (Figure 2). Thus, it is immune to electromagnetic fields, has low power consumption, low-level noise and no need for any electronic filtering [12].

In this paper, we focus on the development of a multi-DoF force sensor for the STIFF-FLOP manipulator and show how to design, calibrate, and calculate a stiffness matrix by considering integration of the sensor with its manipulator.

II. METHODS

A. Design Concept

The design concept of the multi-axial force sensor should satisfy several conditions, which are as follows:

1) The sensor device has to serve as a medium between mutually tangent segments of the STIFF-FLOP manipulator and, hence, should have a ring-like structure to allow pipes for fluidic chambers to pass through proximal segments and reach distal ones.

2) The sensor should be capable of measuring at least three components of external force and moment, namely the longitudinal force, F_z, and the two torques, M_x, and M_y (Figure 3). Note that the STIFF-FLOP manipulator has 3 DoF, including two omni-directional bending motions and one elongation motion.

B. Configuration of Three-Axis Force Sensor

The three-axis force sensor contains three photo interrupters (model SG-105 from KODENSHI CORP.) which are coupled with three mirrors made of write-reflective plastic and a flexible ring-like structure with two plates of ABS plastic (a copolymer of Acrylonitrile, Butadiene, and Styrene) which is designed with a 3D rapid prototyping machine (Figs. 2 and 3). The structure design is based on three flexible cantilever beams measuring the force component F_z (+/- 5N) and two moment components, M_x (+/- 3.5 Ncm) and M_y (+/- 3.5 Ncm).

The photo interrupter consists of a photo diode and a phototransistor, emitting and receiving light, respectively. The amount of light emitted from the photodiode is reflected by the mirror and is received by the photo transistor. The closer the distance between the mirror and the photo interrupter is, the higher the intensity of the reflected light that the phototransistor receives [13]. The amount of reflected light is proportional to the output voltage of the photo interrupter. From the output voltage of the photo interrupter, the distance between the mirror and the photo interrupter can be measured, as shown in Fig. 2 (bottom panels). When an external force F_z and moments M_x and M_y are applied to the upper plate, the three associated cantilever arms are deflected. The three corresponding photo interrupters measure the resultant cantilever arm deflections (δ_1, δ_2, and δ_3) between the upper and bottom plates of the sensor (Fig. 3). In order to anchor the force sensor to the structure of the STIFF-FLOP manipulator, a clocking mechanism is also integrated in the sensor design (Fig. 4). The hollow structure of the whole design and clocking mechanism allows the conveyance of

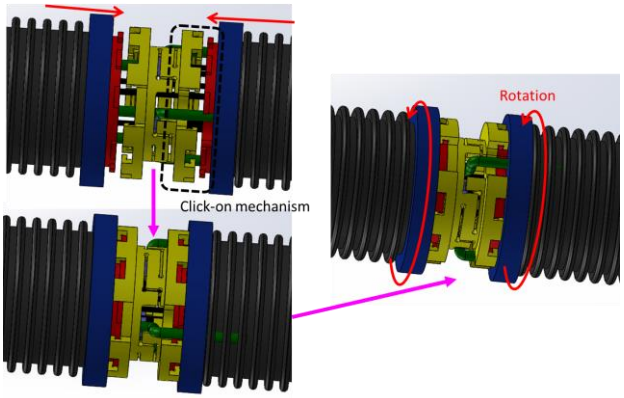

Figure 4. The STIFF-FLOP manipulator and click-on mechanism

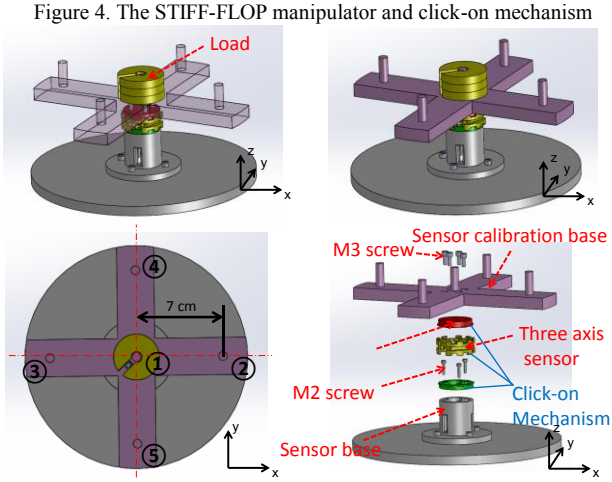

Figure 5. Design of sensor calibration device

TABLE I. EXPERIMEMTAL CONFIGURATION OF THE APPLIED LOADS FOR CALIBRATION

Positions on calibration base (see Fig. 5)	Force and Moment component	Force and Moment ranges
①	$-F_z$	-6N to 0N
②	$-F_z + M_y$	-0.8 to 0 N 0 to5.6Ncm
③	$-F_z - M_y$	-0.8 to 0 N 0 to-5.6Ncm
④	$-F_z + M_x$	-0.8 to 0 N 0 to5.6Ncm
⑤	$-F_z - M_x$	-0.8 to 0 N 0 to-5.6Ncm

optical fibers, electrical wires and air tubes between the different segments of the manipulator with a stable connection of the sensor in between.

III. SENSOR CALIBRATION

A. Setup for Calibration Experiments

In order to use the sensor, a calibration procedure is required. A proper calibration should convert the output voltage of the three photo interrupters into the effective values of the force and torques applied to the sensor. To this aim, a calibration device has been designed, and a stiffness matrix has been calculated, as described below.

1) Calibration device

The device aims at calibrating the normal force F_z and the two moments M_x, and M_y. It consists of a sensor base where

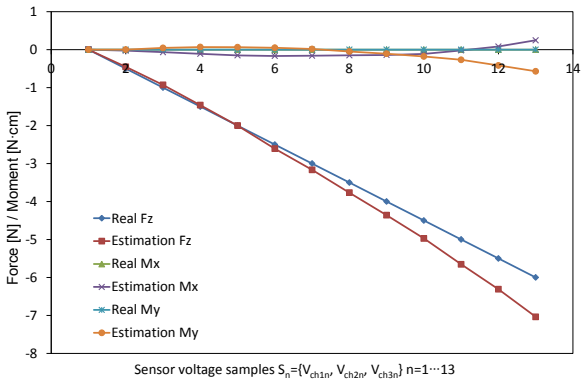

Figure 6. Comparison between real and estimated *Fz* values

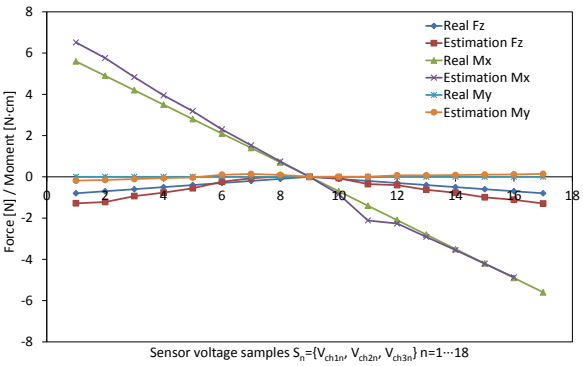

Figure 7. Comparison between real and estimated *Mx* values

the three-axis sensor and the static loads are mounted (Fig. 5). In general, the normal force F_z and the two moments M_x and M_y are coupled when an external load is applied to the sensor, whereas a normal force F_z is fully decoupled from M_x and M_y when the force is applied to the centre of the sensor. For this reason, during calibration, loads are mounted on the base according to the five cases reported in Table 1 (see also Fig. 5). While applying the external loads to the three-axis force sensor, the output voltages of the three photo interrupters are acquired by an analogue-to-digital convertor (ADC) and customized software.

2) Calibration for F_z, M_x, and M_y

A set of loads (from 0 N to -6 N, with steps of -0.5 N) are applied to the sensor calibration base according to configuration (1) in Table 1, and then a set of loads (from 0 N to -0.8 N, with steps of -0.1 N) are applied to the sensor calibration according to configurations (2) through (5) in Table 1, The relationship between F_z and combinations of F_z and M_x, F_z and M_y and output voltages are recorded.

B. Calculation of stiffness matrix by multiple linear regression

The calibration data is used to generate a 3x3 calibration or stiffness matrix, which converts the three output voltages to three physical values of force and torque. Therefore the matrix can be later on multiplied by any three-element voltage vector (column)—see Eq. (1) and (2), below—to obtain the sensor output.

Multiple Linear Regression (MLR) finds the relationship between two or more independent variables and a dependent

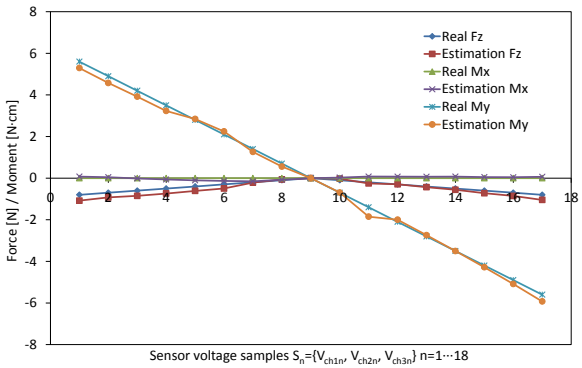

Figure 8. Comparison between real and estimated *My* values

TABLE II. SENSOR ERROR PROPERTY

Force / Moment	Range	Maximum error
Fz [N]	+/- 5.0	0.65 (6.5%)
Mx [Ncm]	+/- 3.5	0.71 (10%)
My [Ncm]	+/- 3.5	0.45 (6.4%)

variable by fitting a linear equation to the observed data. In this implementation, every value of an independent variable, namely each value of the output voltage of the optical fibres, is associated with a value of the dependent variables—i.e., the force F_z and torques M_x and M_y.

By applying MLR, the decoupling stiffness matrix is calculated:

$$\begin{bmatrix} k_{1,1} & k_{1,2} & k_{1,3} \\ k_{2,1} & k_{2,2} & k_{2,3} \\ k_{3,1} & k_{3,2} & k_{3,3} \end{bmatrix} \times \begin{bmatrix} v_1 \\ v_2 \\ v_3 \end{bmatrix} = \begin{bmatrix} F_z \\ M_x \\ M_y \end{bmatrix} \quad (1)$$

$$K = \begin{bmatrix} 2.2284 & 2.4456 & 2.0081 \\ -4.29382 & 2.1929 & 1.7762 \\ 0.0572 & -3.7771 & 2.9985 \end{bmatrix} \quad (2)$$

As shown in Eq. (1) and (2), in the sensor voltage samples v_1, v_2 and v_3, the estimated F_z, M_x and M_y are obtained by using the calculated stiffness matrix. The estimated F_z, M_x and M_y values have errors in comparison with the ground-truth values of F_z, M_x, and M_y, as shown in Figs. 6, 7 and 8. Nevertheless, the calibration matrix can estimate the force and the moments within a sensor range of F_z (± 5 N), M_x (± 3.5 Ncm) and M_y (± 3.5 Ncm) with a maximum absolute and percentage error, as shown in Figs. 6, 7, 8 and Table 2.

IV. CONCLUSION AND FUTURE WORK

In this paper, we have presented a three-axis force sensor using photo interrupters to measure external force and torques of the STIFF-FLOP robot arm. The sensor design enables multi-axis sensing in a multi-segment soft manipulator. We believe that the demonstrated design and solution can be applied to any other soft manipulator where two or more elements are linked via rigid joints. In addition, we have proposed a customized design for sensor calibration and calculated its stiffness matrix by applying a MLR method. Finally, we have validated the sensor range through the experimental measurements.

In future work, sensor characteristics such as error, nonlinearity, crosstalk, repeatability, and hysteresis will be evaluated and improved. Additionally, the force sensor will be integrated within the STIFF-FLOP manipulator to measure external force and momentum components in experimental surgical scenarios. Since the hysteresis level of ABS plastic is likely influential, metallic components such as titanium or aluminium may be used in future versions of the sensor.

REFERENCES

[1] N. Simaan, K. Xu, A. Kapoor, W. Wei, P. Kazanzides, P. Flint, and R. Taylor, "A System for Minimally Invasive Surgery in the Throat and Upper Airways", Int. J. Robotics Research (special issue on medical robotics), vol. 28- 9, pp. 1134-1153, June 2009.

[2] Alexander T. Hillel, Ankur Kapoor, Nabil Simaan, Russell H. Taylor and Paul Flint, "Applications of Robotics for Laryngeal Surgery," Laryngeal Cancer-Otolaryngologic Clinics of North America, Nasir Bhatti & Ralph P. Tufano Eds., Volume 41, Issue 4, pp. 781-791, August 2008.

[3] Zhang J., Bhattacharyya S., Simaan N., "Model and Parameter Identification of Friction During Robotic Insertion of Cochlear-Implant Electrode Arrays," IEEE International Conference on Robotics and Automation (ICRA'2009), pp. 3859-3864, 2009.

[4] D. C. Rucker, B. A. Jones, and R. J. Webster III. "A Geometrically Exact Model for Externally Loaded Concentric Tube Continuum Robots", IEEE Transactions on Robotics, 26(5), pp.769-780, 2010.

[5] N.G. Cheng, M.B. Lobovsky, S.J. Keating, A.M. Setapen, "Design and Analysis of a Robust, Low-cost, Highly Articulated manipulator enabled by jamming of granular media", The 2012 IEEE International Conference on Robotics and Automation (ICRA), pp. 4328–4333, 2012.

[6] A Jiang, G Xynogalas, P Dasgupta, K Althoefer, T Nanayakkara, "Design of a variable stiffness flexible manipulator with composite granular jamming and membrane coupling", 2012 IEEE/RSJ International Conference on Intelligent Robots and Systems (IROS 2012), pp. 2922–2927, 2012.

[7] Arjo J. Loeve, Dick H. Plettenburg, Paul Breedveld, and Jenny Dankelman, "Endoscope Shaft-Rigidity Control Mechanism: "FORGUIDE", IEEE Transactions on on Biomedical Engineering, 59(2), pp.542-551, 2012

[8] M. Cianchetti, T. Ranzani, G. Gerboni, I. De Falco, C. Laschi, A. Menciassi, "STIFF-FLOP Surgical Manipulator: mechanical design and experimental characterization of the single module", IEEE/RSJ 2013 Int. Conf. on Intelligent Robots & Systems, pp. 3576-3581, 2013.

[9] T.C. Searle, K. Althoefer, L. Seneviratne, H. Liu, "An Optical Curvature Sensor for Flexible Manipulators", 2012 IEEE Int. Conf. on Robotics and Automation (ICRA 2012), pp. 4401–4405, 2012.

[10] Y. Noh, S. Sareh, J. Back, H.A. Würdemann, T. Ranzani, E.L. Secco, A. Faragasso, H. Liu, K. Althoefer, "A Three-Axial Body Force Sensor for Flexible Manipulators", 2014 IEEE Int. Conf. on Robotics and Automation (ICRA), pp. 6388-6393, 2014.

[11] S. Sareh, A. Jiang, A. Faragasso, Y. Noh, T. Nanayakkara, P. Dasgupta, L.Seneviratne, H. A. Wurdemann, K. Althoefer, "Bio-Inspired Tactile Sensor Sleeve for Surgical Soft Manipulators", 2014 IEEE Int. Conf. on Robotics & Automation (ICRA), pp. 6388-6393, pp. 1454-1459, 2014.

[12] G. Pallia, S. Pirozzib, "A miniaturized optical force sensor for tendon-driven mechatronic systems: Design and experimental evaluation", Mechatronics, Vol (22), Issue 8, pp. 1097–1111, 2012.

[13] Y. Noh, A. Shimomura, M. Segawa, H. Ishii, J. Solis, A. Takanishi, K. Hatake, "Development of tension/compression detection sensor system designed to acquire quantitative force information while training the airway management task", 2009 IEEE/ASME International Conference on Advanced Intelligent Mechatronics, pp. 1264-1269, 2009.